GISELA LARSSON

Computational studies of early intermediates in the bacteriorhodopsin photocycle

Master's degree project

Molecular Biotechnology Programme

Uppsala University School of Engineering

UPTEC X 01 025	Date of issue 2001-05
Author	
Gisela Larsson	
Title (English)	
Computational studies of early intermediates in the bacteriorhodopsin photocycle	
Title (Swedish)	
Abstract	

We have performed molecular dynamics simulations of the ground-, K- and L-state structures of the bacteriorhodopsin proton pump-cycle, and mapped the hydrogen-bond networks. Our results suggest that the primary proton transfer event is direct and not water mediated.

Keywords	
molecular dynamics simulation, proton transfer, bacteriorhodopsin	
Supervisor	
David van der Spoel **Uppsala University**	
Examiner	
Janos Hajdu **Uppsala University**	

Project name	Sponsors
Language **English**	Security
ISSN 1401-2138	Classification
Supplementary bibliographical information	Pages **29**

Biology Education Centre   Biomedical Center   Husargatan 3 Uppsala

Box 592 S-75124 Uppsala   Tel +46 (0)18 4710000   Fax +46 (0)18 555217

COMPUTATIONAL STUDIES OF EARLY INTERMEDIATES IN THE BACTERIORHODOPSIN PHOTOCYCLE

Gisela Larsson

Sammanfattning

Bakteriorodopsin är ett membran-bundet protein som utnyttjar energin i solljuset till att pumpa en positivt laddad partikel, en proton, från insidan av cellen till utsidan. En laddningspotential skapas som sedan används till att bilda ATP, bakteriens energikälla. Bakteriorodopsin används som modellsystem för bioenergi-processer, men mekanismen är ännu inte helt klarlagd.

En kanal går genom proteinet och i den sitter en rodopsin-molekyl, vilken fungerar som en spärr mellan ut- och insidan av membranet. Överföringen av en proton från ena till andra sidan sker i flera väldefinierade steg, och proteinets olika intermediära tillstånd har identifierats. Vi har med hjälp av datorsimuleringar studerat de tre första intermediärerna och försökt ta reda på i detalj hur protonen flyttas från retinalen till acceptorn, en aspartat-rest längre ner i kanalen. Våra resultat tyder på att protonen går direkt till acceptorn och inte via någon vattenmolekyl eller annan aminosyra-rest, som tidigare föreslagits.

Examensarbete 20 p i Molekylär bioteknikprogrammet

Uppsala universitet Maj 2001

TABLE OF CONTENTS

1. SUMMARY

Bacteriorhodopsin (BR) is a membrane bound protein that uses light energy to pump protons across the bacterial membrane. This creates a proton gradient, which is used to produce ATP. During the process of pumping one proton across the membrane, bacteriorhodopsin goes through several well-characterized intermediate states, which can be distinguished spectroscopically. The three-dimensional structure of the ground-state, as well as of a number of intermediate states, are available. However, the mechanism of pumping is still not resolved.

In this work we have focused on trying to understand the role of internal water molecules in the primary proton transfer event, using molecular dynamics simulations. Our models are based on crystal structures of the ground-state and of the early photo intermediates K and L, with additional water molecules introduced into the protein channels. From the 200-500 ps long simulations we have created an average structure of each state and described the hydrogen bonding networks. We show that the patterns are very different between the three states, supporting the view that internal water movements are important for proton transfer. We cannot, however, see a continuous proton path in any of the average structures. Regarding the question of whether the primary proton transfer between the protonated Schiff base and an aspartic acid residue is direct or water mediated, our results support a direct transfer. We see a considerable flex-movement of the Schiff base towards the aspartic acid in the L-state simulation, creating the opportunity for direct transfer.

2. INTRODUCTION

2.1. Bacteriorhodopsin

BR is a light driven proton pump, and has long been viewed as the simplest molecule to perform the task of transporting ions across the membrane. It has therefore been used as a model system for membrane proteins in general and transporters in particular. The transport of ions against an electrochemical potential is a fundamental process to all forms of life. In the case of BR, the energy of green light (500-650 nm) is converted to a proton gradient (up to 250 mV), which is then used to produce ATP, providing the cell with energy (Kühlbrandt 2000).

BR is a 26 kD protein found in the purple membrane of the archaebacterium *Halophilic salinarium*, an organism thriving in high temperature saturated salt brines that are exposed to bright sunlight. BR consists of seven transmembrane helices (A to G) tightly surrounding a retinal molecule, the light absorbing chromophore. The retinal is covalently attached to the protein through a Schiff base linkage to a lysine residue (K216) on helix G. A cross section of BR with residues important for proton transfer is shown in figure 1. The retinal molecule divides

1

the protein channel into two halves, one cytoplasmic (CP) and one extracellular (EC) side. Both half channels are lined with residues crucial for proton transport, in particular D96 on the CP side and D85 on the EC side (Hauputs et al. 1999).
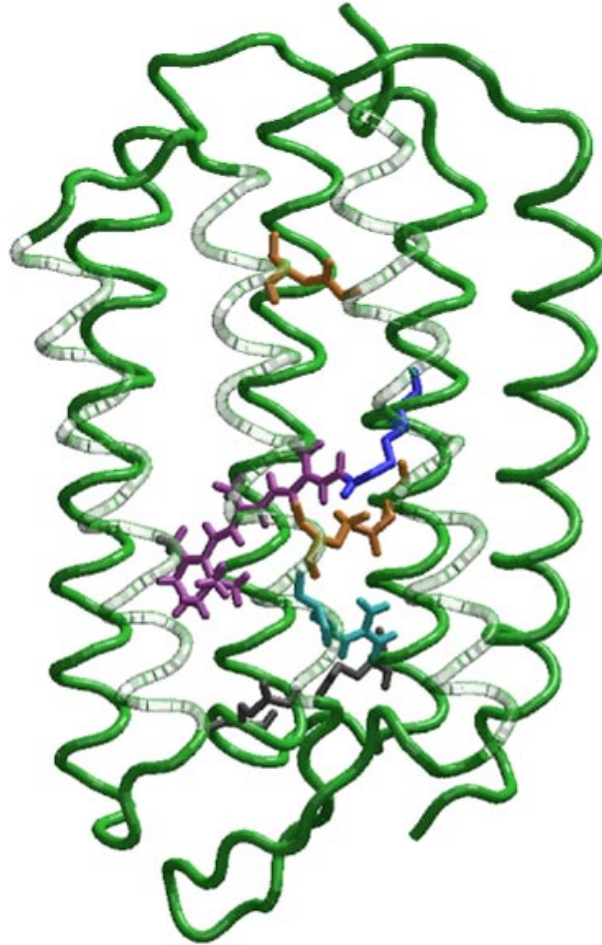

Figure 1. Bacteriorhodopsin with the retinal molecule in light purple and K216 in dark purple. Other residues important for proton transfer are the aspartic acids D96, D85 and D212 (orange), the arginine R82 (light blue) and glutamic acids E194 and 204 (grey).

2.2. The Photocycle

Absorption of a photon, isomerizing the retinal molecule from an all *-trans* to a 13- *cis* conformation, initiates the catalytic cycle (termed photocycle) and triggers the vectorial transport of one proton from the cytoplasmic to the extracellular side, that is, from the inside to the outside of the cell. The retinal then reverts back to its all-*trans* form spontaneously, completing the cycle. An approximate photocycle can be described by the scheme bR$\leftrightarrow$bR*$\rightarrow$J$\rightarrow$K$\leftrightarrow$L$\leftrightarrow$M$_1$$\rightarrow$M$_2$$\leftrightarrow$N$\leftrightarrow$O$\rightarrow$bR (see figure 2), where bR denotes ground-state

BR, bR* after the up-take of a photon, and J to O the respective intermediate states. The different states have been characterised spectroscopically (Hauputs et al. 1999), the subscripts in figure 2 indicate their maximum absorption wavelengths. The nature of the J intermediate is unknown. In the K-state the retinal has adopted its 13-*cis* conformation. The torsion of the retinal polyene chain relaxes in the K to L transition, and the displacement of the Schiff base disrupts the hydrogen-bonding network and destabilises the separated charges at the active site. In the L to M_1 transition pK_a-shifts of the Schiff base and D85 induce protonation equilibrium between the two (reviewed in Hauputs et al. 1999). A shift of this equilibrium then leads to protonation of D85, linked to the release of a proton on the extracellular side of BR, occurring in the M_1 to M_2 transition. The N intermediate is formed after reprotonation of the Schiff base, induced by conformational changes in the cytoplasmic region. The next step of the cycle (N to O) is reprotonation of D96 from the cytoplasmic side, as well as re-isomerization of the retinal to a twisted all-*trans* conformation. Deprotonation of D85 and relaxation of the retinal in the O to bR transition re-establishes the ground state, and the photocycle is repeated. Tremendous efforts have been made, using a variety of biophysical methods, to determine the exact nature of each intermediate, and relate the changes in every step to the transport function.

2.2.1. Ground state

The structure of BR was first determined in 1975 by Henderson and co-workers (Henderson et al. 1975) using cryo-electron microscopy of two-dimensional crystals that form in the cell membrane. Since then, high-resolution x-ray and cryo-electron microscopy structures have revealed a more detailed structure of ground state BR (for example Luecke et al. 1999a), as well as of intermediates K (Edman et al. 1999), L (Royant et al. 2000), M (Luecke et al. 1999b, Sass et al. 2000) and N (Vonck 2000). Each BR molecule contains a bundle of seven helices surrounding a retinal chromophore. In the ground state structure the all-*trans* retinal is linked via a protonated Schiff base to K216, and is flanked by the proton donor and acceptor, D85 and D96, on its extracellular and cytoplasmic sides, respectively. The extracellular region also contains the hydrophilic residues D212, R82, E194 and E204, shown to be involved in the proton transfer process (Lanyi 1999). Recent crystal structures have also shown numerous water molecules on the extracellular side (Luecke et al. 1999a) which, together with the polar residues, form an extensive hydrogen-bonding network. The cytoplasmic half of the protein pore lacks such a well-defined network, and a protein transport pathway is believed to form and reform with water rearrangements. Proton capture from the cytoplasmic bulk is mediated by the excess of negatively charged surface groups and phospho head-groups of tightly bound lipids. These phospholipids are believed to have a specific role in maintaining BR's functionality (Hauputs et al. 1999). The active site includes a well-resolved water molecule, W402, co-ordinated between the Schiff base and the two aspartic acids, D85 and D212 (figure 3), believed to help stabilise the separated charges.
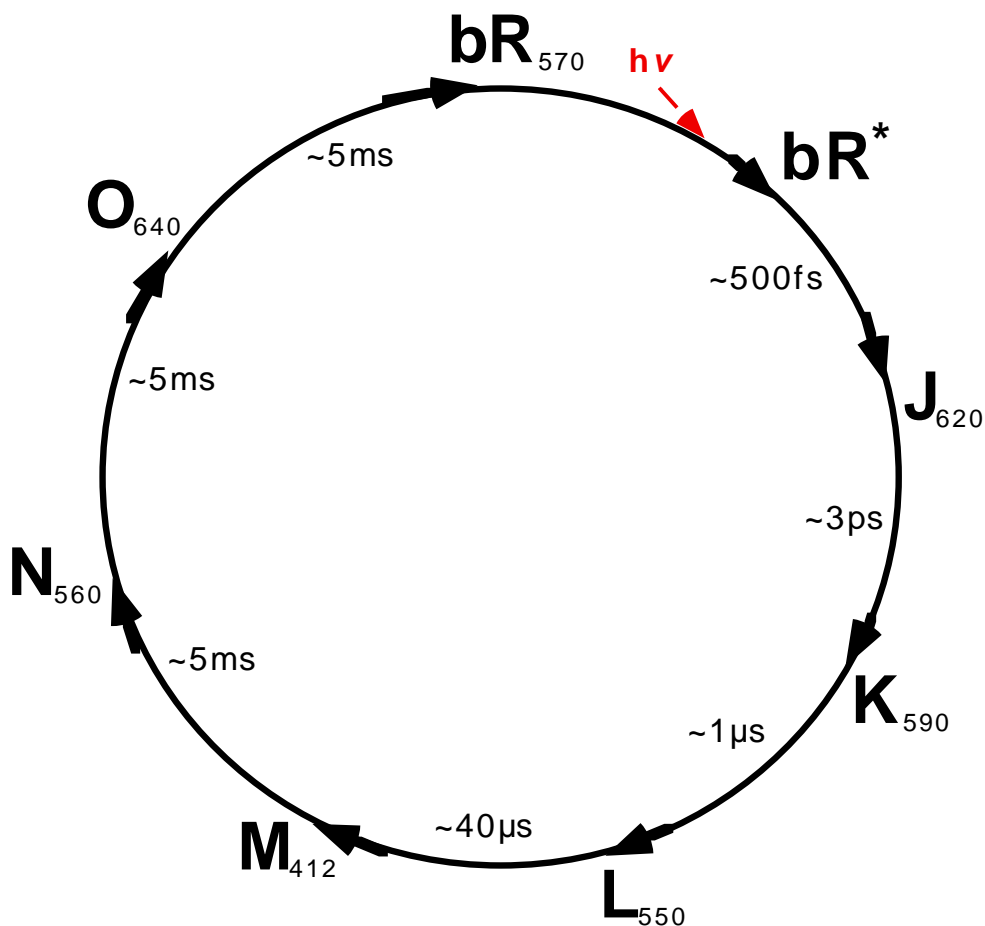
Figure 2. The bacteriorhodopsin photocycle with intermediates J, K, L, M, N and O indicated.

2.2.2. Primary photo events and the J intermediate

The uptake of a photon by ground state bacteriorhodopsin generates the excited state bR*, with a lifetime of about 200 fs. bR* successively decays to the intermediates J_{625} and K_{590}, the latter being a ground state product with a 13-*cis* retinal. Two different models for the primary photoreaction exist; the two-state and the tree-state model. The two-state model postulates that electrons are excited from the ground state surface, S_0, to the excited state surface, S_1. The wave package develops for some time and then returns to the ground state following a barrierless reaction scheme. This model does not, however, agree with some more recent time-resolved absorbance measurements, leading to the suggestion of a three-state model with electronic surfaces S_0, S_1 and S_2. Quantum chemical calculations using the three-state model on a retinal analogue have been able to explain the experimental data (Humphrey et al. 1998). The simulations reproduce the observed quantum yield of 0.64, and predict the time needed to pass the two crossings along the reaction co-ordinates, the S_1 to S_2 crossing after a 30° torsion, and S_2 to S_0 after a torsion of 90°. The nature of the J intermediate is still unknown, the brief halt at the

S_2 to S_0 crossing points makes it unlikely that it can be identified as the J-state. There is even disagreement to whether the J-state is an electronically excited state, or a ground state intermediate.

2.2.3. K intermediate

The K-state is the earliest intermediate of the BR photocycle for which a structure has been determined (Edman et al. 1999), to a resolution of 2.1 Å. Crystals grown in lipid cubic phase were illuminated with green light at 110 K, making it possible to trap the accumulated early intermediate. Single crystal microspectrophotometry was used to characterise the trapped ground and intermediate states, the latter identified as the low temperature K (K_{LT}) intermediate. Both K_{LT} and K show a red shift in the absorption maximum compared with the ground state spectrum, from 570 nm to 590 nm. K_{LT} and K differ in that the 13-*cis* retinal geometry is slightly distorted for K_{LT}, and planar in the case of K (Braiman and Mathies 1982). The structural rearrangements following the ground- to K-state transition are confined to the vicinity of the chromophore. Changes in the orientation of the Schiff base perturbate the hydrogen-bonding network of helix G, centred on K216, and also dislocate a key water molecule, W402. Residues D85 and D212 are pulled together by the retinal, moving closer to the Schiff base. This probably leads to an increase in the pK_a of D85. Another effect of the retinal isomerization is an upward movement of the indole ring of adjacent residue W182. A second water molecule (W401), hydrogen-bonded to D85 in the ground state structure, is partially disordered. Movements along the isomerized retinal chain could not be observed in the K_{LT}-state due to increased disorder.

2.2.4. L intermediate

Using the same technique as in the case of the K intermediate, the L-state structure was recently determined (Royant et al. 2000). It is shown that the early movements around the active site have propagated towards the extracellular surface and new structural rearrangements appear. Water 401 and 400 are dislocated, one of them (referred to as W401 by the authors) reappearing in an intermediate position (see figure 3). This disruption allows movement of helix C, resulting in the primary proton acceptor D85 moving closer to D212 and the Schiff base. It should be pointed out that the Schiff base proton is pointing away from D85 towards the CP side, in the K- as well as the L-state structure. Deformation of helix G has evolved to the cytoplasmic side of the active site, facilitating significant movements of helices F and G later in the photocycle. Also, the orientation of R82 is flipped, approaching E194, which is part of the leaving group, anticipating the release of a proton to the extracellular medium.
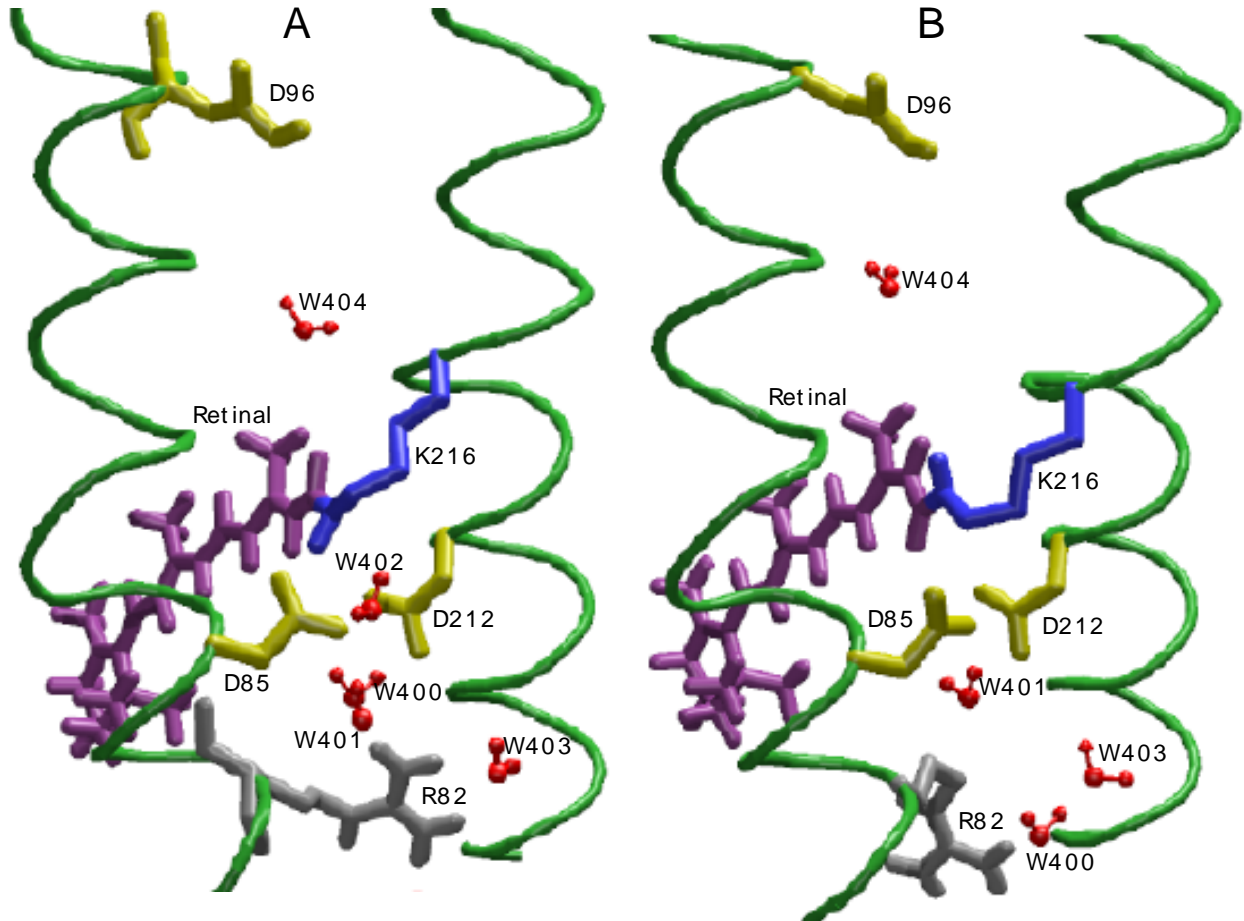
Figure 3. Close-up of the retinal surroundings in ground-state (A) and L-state (B) bacteriorhodopsin. Helices C and G are shown.

2.2.5. M intermediate

The M-state is a key intermediate in the photocycle. In the L to M transition a proton is transferred from the Schiff base to the primary acceptor, D85, and during the M-state a proton is released to the outside of the cell. To assure vectorial proton transport, de- and reprotonation of the Schiff base must occur from different sides of the membrane, i.e. there is need for a switch mechanism. This means that at least two different M intermediates must exist, differing in accessibility of the Schiff base. The two M-states are termed M_{ec} and M_{cp} for extracellular and cytoplasmic side, respectively (Haupts et al. 1999). The existence of several M species has been recognised for a long time as the intermediate rises and decays with more than one time constant. In the literature the two M-states are usually referred to as M_1 and M_2, it is not clear whether these two intermediates are identical to M_{ec} and M_{cp}. To make it more confusing, the notation M_N is sometimes used for a late M-state with the protein in the conformation of the N intermediate, but where the Schiff base has not yet been reprotonated. The M_N state has been trapped in the D96N mutant (in wild type BR the Schiff base is reprotonated by D96), but whether M_N is a

transient intermediate of the catalytic cycle of wild type BR, or is specific for the mutant is not known.

Crystallographic studies on trapped M intermediates have been successfully carried out using mutants in combination with low temperature (Luecke et al. 2000, Luecke et al. 1999b), cryo-trapping of the wild type enzyme (Sass et al. 2000) and electron crystallography of a triple mutant (Subramaniam and Henderson 2000). A rather fierce debate is going on regarding the quality and the interpretation of the different structures, but there is agreement on what the key features are. The largest conformational changes in the late M-state can be seen on the cytoplasmic side of the protein pore. The top (cytoplasmic) ends of helices F and G move, enlarging the cytoplasmic pore and enabling in- and outward diffusion of water molecules (Subramaniam and Henderson 2000). Reprotonation of the Schiff base requires a hydrogen-bond network in the cytoplasmic channel, made up by side-chains and water molecules. However, a continuous water string below or above D96 has not been seen in any of the structures. Rearrangements of waters have been suggested to be the rate-limiting step in producing the N-state. An alternative to a continuous water channel is a directed random walk by one water molecule through the pore (Sass et al. 2000).

The positively charged side-chain of R82 in the extracellular half of the pore is displaced towards the leaving group, a movement already predicted by theoretical calculations (Sass et al. 2000). This is true also in the case of the D96 mutant, indicating that R82 is the agent of coupling between protonation of D85 and deprotonation of the release group (Herberle et al. 2000, Luecke et al. 2000). What is also under debate is which residue is responsible for the final proton release. Mutation of either E194 or E204 alters release kinetics, but the protonation state of neither changes during the photo cycle, according to time resolved FTIR experiments. The strong hydrogen-bond interaction between R82 and E204 makes this glutamate a likely candidate, and the strong interaction could, according to Sass, explain why no pronounced difference band was observed in FTIR spectra (Sass et al. 2000, Herberle et al. 2000).

The exact nature of the switch mechanism is still unknown. It seems likely that it is partly governed by protein conformational changes and partly by the isomerization of retinal. Another intriguing question also remains to be answered; how does the primary proton transfer take place? There is disagreement regarding whether the proton exchange between the Schiff base and D85 is direct or mediated by a water molecule or residue sidechain. A direct transfer requires that the Schiff base N-H bond points, at least partially, toward D85 and not toward the cytoplasmic side. This model is supported by the single step kinetics of the reaction. The water mediated model suggests a dissociation of W402 (located between the Schiff base, D85 and D212) to protonate D85, and the hydroxyl ion produced could move to the cytoplasmic side of the Schiff base and receive its proton (Luecke et al. 2000). This ion transfer is similar to that of halorhodopsin. It does not, however, agree with the fact that W402 is not seen in the K-state

structure (Edman et al. 1999). Henderson (Henderson et al. 2000) has proposed a model where the proton reaches D85 via T89.

2.2.6. Completing the cycle

The key feature of the M to N transition is the proton transfer from D96 to the Schiff base. It is clear that the N-state, shown to have the retinal molecule in a 13-*cis* configuration, must include two substates as reprotonation of D96 from the cytoplasm occurs during the lifetime of this intermediate (Haupts et al. 1999). Structurally, the N-state exhibits largely the same features as the late M-state. In the transition of the N- to O-state, D96 is reprotonated from the cytoplasmic side and the retinal is converted back to its all-*trans* form. The exact time point of reisomerization of retinal in wild type BR is not known. In the last step of the photocycle D85 is deprotonated and the protein conformation returns to its initial state.

2.3. Theoretical Studies

BR is also a popular target for theoretical calculations. A variety of methods have been used, including molecular dynamics simulations, quantum mechanics calculations, and combined quantum/classical approaches. The photoisomerization process has been investigated , as well as the dynamic behaviour of the retinal Schiff base in different stages of the photocycle.

Considering the high expenses/long calculation times required by most theoretical methods it is important to make the model system as simple as possible, while retaining optimal accuracy. Suhai and co-workers have studied how much of the polyene chain it is necessary to include to get a realistic model for quantum calculations (Tajkhorshid et al. 1997), and what effect the retinal methyl groups have on the chromophore (Tajkhorshid and Suhai 1999b). The free electron pairs of the polyene chain double bonds are distributed along the chain creating a conjugated electronic structure. The results of the density functional theory (DFT) calculations performed show that a longer conjugated system has a positive effect on the proton affinity of the Schiff base. Using the same method, it was concluded that the location and amount of twist in the retinal backbone can be manipulated by the protein environment via steric interactions between the methyl groups and the protein binding-pocket. This influences the pK_a of the Schiff base group, implying that the backbone geometry is important for proper proton transfer. In another study the investigators looked at how the electronic structure of the chromophore is effected by the protein environment (Tajkhorshid and Suhai 1999a). The effects of surrounding polar and/or polarizable amino acids with at least one heavy atom within 5 Å of the retinal Schiff base were investigated, as well as that of the water molecule (W402) hydrogen-bonded to the Schiff base group. Due to the size of the system, the effect of each amino acid had to be considered separately. The results show that only charged residues, namely Asp85 and Asp212, and W402 significantly influence the structure and charge distribution of the polyene. These

three groups seem to restore, to some extent, the bond alternation between single and double bonds along the conjugated chain.

The photoisomerization of retinal has been investigated extensively by Schulten and co-workers through molecular dynamics simulations (Humphrey et al. 1995, Humphrey and Schulten 1997). The aim has been to compare the different possible photoproducts and determine which one most closely resembles the actual structure of BR during the early steps of the photocycle, that is the structure of the K_{590} intermediate. Simulations were carried out on schematic potential surfaces describing the ground and excited states of retinal with a second potential bias to account for the fact that the crossing point of the two surfaces seem to favour the direction all-*trans*→13-*cis*. The results (Humphrey et al. 1995) indicated that the quantum yield of BR's phototransformation (which has been determined to 0.64 ± 0.04) is controlled by the crossing from retinal's excited state to its ground state surface. The authors propose the so-called case two product, with a highly twisted C_6-C_7 bond in the retinal and with the Schiff base proton oriented perpendicular to the membrane normal, to represent the K-state structure. This orientation of the proton would provide a pathway for proton transfer to D85, as opposed to the case one product where the Schiff base proton points toward the cytoplasmic side. They cannot, however, account for the low yield of case two photoproducts relative to case one products. The authors suggest that W402 is crucial for proton transfer, acting as a mediator between the Schiff base and D85. This clearly disagrees with the structure of the K-state, where W402 is dislocated (Edman et al. 1999). Later a similar study was performed on the wild type and a set of mutant proteins (Humphrey et al. 1997), with the result that no case two products were formed when simulating inactive mutants. They see this as support for their earlier suggestion that only case two photoproducts initiate a functional pump cycle.

Recently, molecular dynamics simulations were performed on a model of BR in its native environment, the purple membrane (Baudry et al. 2000). A key advance with this study is the integration of atomic detailed BR structures into a model for the entire membrane, based on information from several crystal structures. Internal water molecules were placed in the protein pores using free energy perturbation theory, agreeing well with positions of crystallographic waters, to predict water movement during the photocycle. They can show that waters are displaced, supporting the idea that this is crucial for proton pumping. The photoreaction of retinal from an all-*trans* to a 13-*cis* conformation in the protein is far more selective and efficient than photoreactions of retinal in solution (Hermone and Kuczera 1998), indicating the importance of studying BR in its native environment.

2.4. This Study

An efficient ion pump has to overcome two fundamental problems; (a) how to conserve and transmit excess free energy within the protein, and (b) how to alternate access of the ion binding site to the two membrane surfaces during the transport cycle. In the case of BR a model is emerging for how this is done, regarding the energetics as well as the mechanism of transport. The energy gained from light is initially stored in the form of a steric and electrostatic conflict between the photoisomerized chromophore and its binding pocket. Later the excess energy spreads to more remote parts of the protein (Lanyi 1999). A key to understanding the energetics of the system is to elucidate how the proton moves from the Schiff base nitrogen to the primary proton acceptor, D85. The second question of importance is the access change in the channel, making the reaction unidirectional. This switch is believed to be governed by pK_a-changes in the retinal moiety, and the making and breaking of hydrogen-bonds in the extracellular and cytoplasmic directions (Hauputs et al. 1999). In this study we have focused on trying to understand the primary proton transfer, using molecular dynamics simulations.

A prerequisite to perform relevant simulations is the availability of high-resolution structures. There is a wild type K intermediate structure (Edman et al. 1999) and several M-state structures, of wild type enzyme as well as of mutants (Luecke et al. 2000, Luecke et al. 1999b, Sass et al. 2000 and Subramaniam and Henderson 2000). Recently, also the L-state structure was published (Royant et al. 2000). Even with this new information on the L- and M-state structures, it is not possible to determine how the primary proton transfer takes place. One problem is of course that x-rays do not see protons at this resolution. There is disagreement on whether the proton moves directly from the Schiff base to D85, or via a water molecule. No such water molecule, situated between the donor and the acceptor, could be resolved in the L intermediate. However, the distance between the two groups (about 4.5 Å) seems too large for a direct transfer, and the angle is not favourable. It might be that the transfer is water mediated but the water fluctuates a lot. In that case, molecular dynamics simulations can predict the presence of such a water molecule. Simulations can also give a clue to whether fluctuations of D85 and the Schiff base are large enough to allow a direct transfer.

We have performed 200 to 500 ps long simulations of the ground, K and L intermediates, using available crystal structures as starting points. Crystallographic water molecules, as well as additional low energy waters, were included in the simulations to trace water movements in the protein channel in the different states. To get a more realistic model, we inserted the protein in a slab of argon atoms, mimicking the hydrophobic membrane environment, and surrounded the system with water molecules (figure 4). Waters were then able to diffuse in and out of the protein pore, a feature believed to be important for the function of BR (Baudry et al. 2000). Our data provides information about the hydrogen-bond patterns for the three different states, and insights into the primary proton transfer.

3. THEORY

3.1 Computational Chemistry

Computational chemistry is focused on solving chemical problems by calculations based on theoretical methods. These methods have numerous applications, for example the design of new materials or the investigation of binding properties of a ligand to an enzyme. Describing the potential energy surface, that is the energy as a function of the nuclear co-ordinates, provides useful chemical information. The link between properties of individual molecules and the macroscopic observable is statistical mechanics.

There are different methods to describe the potential energy surface. Quantum mechanic methods, also called electronic structure methods, give the most detailed description of the electron distribution. The aim is to determine the electronic wave function, i.e. to solve the Schrödinger equation. In density functional theory methods the correlation between electron density and energy is used. A less expensive approach is to use molecular mechanics, also called force field methods, where the quantum aspects of the nuclear motion are neglected. This means that the dynamics of the atoms is treated by classical mechanics, and the Schrödinger equation does not have to be solved.

3.1.1. Statistical mechanics

Solvation plays a crucial role in determining the properties of molecules, as biologically relevant processes occur in aqueous systems under rather specific pH and ionic conditions. The dielectric constant of the media surrounding a macromolecule clearly affects its conformation. It is therefore important to understand solvation effects to address the fundamental question of how a protein's particular three-dimensional structure is determined by its sequence. There are various methods of treating solvation, ranging from a detailed description at the molecular level to reaction field methods where the solvent is modelled as a continuous medium.

To model macroscopic properties it is necessary to generate an ensemble of molecules. Such a collection of conformational states can then be averaged and compared with experimental results. There are two major techniques to produce a representative ensemble; Monte Carlo (MC) and Molecular Dynamics (MD).

In the MC method a sequence of conformations is generated from an initial geometry by picking a random molecule, translating it in three dimentions and rotating it around an axis. The new geometry is accepted immediately if it is lower in energy, and if it is higher in energy it is accepted if it's Boltzmann probability, $\exp(-\Delta E/k_B T)$, is higher than a randomly generated number between zero and one. If the geometry is rejected the system is returned to its previous state. The system is not constrained by barriers on a potential surface, making MC calculations especially useful when investigating properties of small molecules in solution. The MC method

is not suitable for simulations of larger molecular systems with cooperative movements, e.g. a protein, nor the analysis of dynamic events and non-equilibrium behaviour, as no forces are generated.

The second method is MD, simulating the natural motions of molecules. A series of time-correlated points in phase space are generated, resulting in a trajectory with successive conformations of the system. The starting co-ordinates and velocities are propagated according to Newton's second equation, $\mathbf{F}=m\mathbf{a}$ (where $\mathbf{F}$ is the force vector, m the particle mass and $\mathbf{a}$ the acceleration vector), by a series of small time steps. MD is the method of choice for observing time-dependent properties, such as protein folding. For these calculations a model of the force field, which governs motion, is necessary.

3.1.2. Force field

In MD simulations, the force $\mathbf{F}$ exerted on an atom is computed from the derivative of the potential energy, $U(\mathbf{r})$, with respect to the co-ordinates of the atom, $\mathbf{r}$:

$\mathbf{F} = -dU(\mathbf{r})/d\mathbf{r} = m*d^2\mathbf{r}/dt^2$

$U(\mathbf{r})$ is calculated using a molecular mechanics force field, consisting of a set of equations called the potential functions, and a set of parameters, experimentally or theoretically determined. A force field consists of three parts; (i) non-bonded interactions, (ii) bonded interactions and (iii) special interactions.

(i) The non-bonded interactions consist of the van der Waals interactions, usually modelled by a Lennard-Jones (LJ) potential, and the electrostatic interactions, described by a Coulomb potential. All interactions between different molecules or between atoms separated by at least three bonds are calculated.

The LJ potential between two atoms i and j equals:

$U_{LJ}(r(ij)) = 4\,\varepsilon(ij)\,[\,(\sigma(ij)/r(ij))^{12} - (\sigma(ij)/r(ij))^6\,]$

where $r(ij)$ is the distance between atom i and atom j, ε is the well depth of the energy minimum and σ is the Van der Waals radius. The attractive term is due to electron correlation, referred to as dispersive or London forces, which is an induced dipole-dipole interaction, and decreases as r^{-6}. The repulsive term is due to the overlap of the electron clouds of two closely positioned atoms (the Pauli Principle), and decreases as r^{-12}. The repulsive part is not exactly r^{-12} but this description saves computational effort, as $r^{-12} = (r^{-6})^2$.

The LJ parameters are constructed using the combination rules

$\sigma(ij) = 1/2*(\sigma(ii) + \sigma(jj))$

$\varepsilon(ij) = (\varepsilon(ii)* \varepsilon(jj))^{1/2}$

The Coulomb interaction between two charged particles is:

$U_C(\mathbf{r}(ij)) = 1/(4*\pi*\varepsilon_0)\,[\,q(i)q(j)/\varepsilon_r*r(ij)\,]$

where q is the partial charge of the atom, ε_0 is the permittivity in vacuum, and ε_r is the dielectric constant of the medium. The partial charges of each atom in the system can be assigned through quantum chemistry calculations. The Coulomb interactions are long ranged, decaying as r^{-1}, and to reduce computational costs they are usually approximated with a constant dielectric environment beyond a certain cut-off value. To get rid of truncated forces at the cut-off radius, the potential can be modified by a shift function, in combination with Ewald or Particle-mesh Ewald (PME) summation, to include all interactions.

(ii) The bonded interaction terms are bond-stretching, angle-bending and dihedrals.
The bond-stretching (U_B) and the angle-bending (U_a) are usually represented by harmonic potentials:
$$U_B\,(r(ij)) = 1/2*k^{\,b}(ij)*[r(ij) - b(ij)]^{\,2}$$
$$U_a\,(r(ijk)) = 1/2*k^{\theta}(ijk)*[\theta(ijk) - \theta^0(ijk)]^2$$
The dihedrals can be described as a periodic function of the form:
$$U_d\,(\phi\,(ijkl)) = k^{\phi}*[1+\cos(n*\phi - \phi_0)]$$
Above, k(ij) is the force constant for the bond, angle and dihedral, respectively, b the bond length, θ the angle and ϕ the torsion angle, n is the multiplicity. k^b and k^{θ} are determined spectroscopically, and k^{ϕ} by quantum mechanical calculations.
The dihedral angle interactions can also include an improper dihedral term, used for example to keep the planarity of aromatic rings.

(iii) Special interactions are not really part of the force field, but will contribute to the potential function, if used. They include position-, angle- and distance restraints, and are used to reduce phase space and concentrate the conformational sampling around a likely structure, e.g. if experimental data is available.

4. METHODS

Molecular modelling is a way to describe complex chemical systems in terms of a realistic and functional model. The aim is to understand and predict macromolecular properties based on detailed knowledge on an atomic scale. Naturally, the reliability of the result depends on the accuracy of the model, including the force fields.

4.1. Building the Models

4.1.1. Protein

High-resolution crystal structures were used as starting structures for the molecular dynamics simulations. The following structures were used: PDB entry 1QHJ for the ground state simulations (Belrhali et al. 1999), 1QKB for the K-state (Edman et al. 1999), and 1EOP for the L-state (Royant et al. 2000). The structures are refined to 1.9, 2.1, and 2.1 Å, respectively. In all cases crystallographically resolved water molecules were included in the models. To make the amino acid sequence identical for the three starting structures, the following residues were mutated to alanines; M163, R227 and E232. These residues are not believed to be involved directly in the proton pumping.

4.1.2. Internal water molecules

To add water molecules manually, or with a computer program, to a crystal structure can be a good strategy as all water molecules might not be resolved crystallographically because of high thermal mobility. Additional internal waters were introduced in our models at energetically favourable positions using the program Dowser by Hermans et al. (hermans@med.unc.edu). With Dowser a molecular surface is constructed from the input structure file, producing positions at which a solvent probe (with default radius 0.2 Å) touches three protein atoms simultaneously. The surface is then sorted into buried and exposed water positions, and the exposed ones are disposed of. Energies are computed for the best placement of the buried waters, and low-energy positions below a typical cut-off value of $-10kcal*mol^{-1}$, are given.

For the placement of additional internal water molecules in our models the structure files described above were used as input. The retinal molecule parameters were included as a separate descriptor file. A probe with radius 0.2 Å was used, but the energy cut-off was modified to a less stringent $-2kcal*mol^{-1}$. Waters introduced by Dowser are denoted D and the crystallographically resolved water molecules W.

4.1.3. Protein environment

It was desirable to mimic the natural environment of the protein as close as possible, without increasing the size and complexity of the system too much. The hydrophobicity of the membrane was described in the form of low temperature argon atoms, composing a "membrane slab" into which the protein was fused. The construct was then solvated in a rectangular box of 7*7*7 nm filled with 5,983 single point charge water molecules (Berendsen et al. 1981). The system can be viewed in figure 4. Solvation was performed, as well as all the simulations, using the chemical simulation software package GROMACS (van der Spoel et al. 1996).
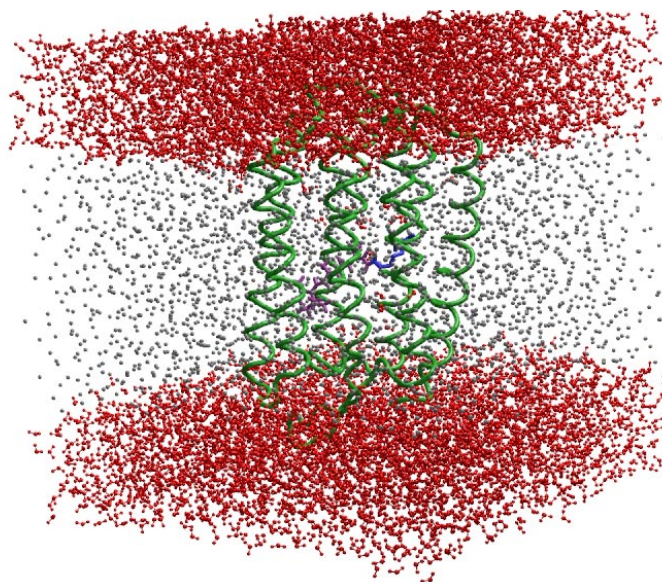
Figure 4. The model used for molecular dynamics simulations with water molecules in red, argon atoms in grey and the protein molecule in green.

4.1.4. Molecular dynamics

Residues D96 and D115 have been shown, both experimentally by Fourier transform infrared spectroscopy (Gerwert et al. 1989) and through theoretical studies with a macroscopic dielectric model (Bashford and Gerwert1992), to be protonated. All other residues were kept at their natural protonation state at pH 7, which is a simplification as there is a pH-gradient of about four units across the membrane.

The solvated protein was minimised using the steepest descent algorithm for 1000 steps. Equilibration of the system was done with a restrained MD run of 20 ps to allow the argon and water molecules to relax. All protein heavy atoms were restrained to their crystal positions with a force constant of 1000 kJ*mol^{-1}*nm^{-1} and kept at 300 K, while the temperature of the argon and water molecules was 120 K. The temperatures were controlled for protein, solvent and argon molecules separately, using weak coupling to a bath of constant temperature (Berendsen et al. 1984), with a coupling constant τ_T of 0.1 ps. The pressure was controlled, in the equilibration runs as well as the production runs, using an-isotropic weak coupling to a bath of constant pressure (1 bar) with a coupling constant τ_P of 4 ps in all directions. All simulations were done using periodic boundary conditions. The centre of mass motion was removed in every step. The coulomb interactions were given by PME electrostatics (Darden et al. 1993) with a cut-off of 0.8 nm, a grid spacing of 0.1 nm and cubic interpolation order. A group based twin-range cut-off of 1.4 nm for van der Waals interactions was used. The dielectric constant, $\varepsilon=\varepsilon_0*\varepsilon_r$, was set to $\varepsilon=\varepsilon_0$, i.e. $\varepsilon_r=1$. The time step was 1 fs and a neighbour list up-date was done every fifth step. All bonds were constrained using the Lincs algorithm (Hess et al. 1997). The Gromos-96 43a1 forcefield was used (van Gunsteren et al. 1996) modified to include parameters for the retinal and the Schiff base, where the partial charges were kindly provided by Emad Tajkorshid (Tajkorshid et

al. 1999b, personal communication), and the geometry taken from the crystal structures. The argon - water oxygen Lennard-Jones parameters were modified to $\sigma=0.36$ nm and $\varepsilon=0.84$ kJ*mol^{-1} to keep water molecules from diffusing into the membrane. Production simulations of 200 to 500 ps were done with the equilibrated systems as input. The temperature was kept at 300 for the protein and solvent, and 5 K for the argon molecules, with coupling constant $\tau_T=0.1$ ps. The protein C_α atoms were restrained to their crystal positions by a force constant of 100 kJ*mol^{-1}*nm^{-1}. All other parameters were the same as for the equilibrations.

4.1.5. Analysis

500 structures in the 150 to 200 ps section of the trajectories of the ground-, K- and L-state production simulations were averaged and minimised for 1000 steps (as above) for analysis. Potential hydrogen-bonds were analysed by GROMACS (van der Spoel et al. 1996), with acceptor-hydrogen distance < 2.5 Å and donor-hydrogen-acceptor angle > 120°. The figures were plotted using VMD (Humphrey et al. 1996) and Raster3D (Merritt et al. 1997).

5. RESULTS AND DISCUSSION

5.1. Stability

The stability of the system was initially a problem due to water molecules that had diffused into the membrane. This was taken care of by reducing the time-step from 2 fs to 1 fs, and by a modification of the Lennard-Jones parameters for the argon - water oxygen interaction to $\sigma=0.36$ nm and $\varepsilon=0.84$ kJ*mol^{-1}. This increased the repulsion between argon and water, and the two layers were kept separated.

Equilibration of the systems for 20 ps resulted in models with well relaxed argon and water molecules. The potential energy of the different structures in the production runs converged within about 80 ps, and a 200 ps trajectory is therefore sufficient to look at side chain and water movements. Figure 5 shows the potential energy over time in a K-state simulation. Also, the root mean square deviation of the trajectory structures from the crystal structure over time was calculated (figure 6), giving an average deviation of 1.0 Å for the 100 to 300 ps section of a K-state simulation.
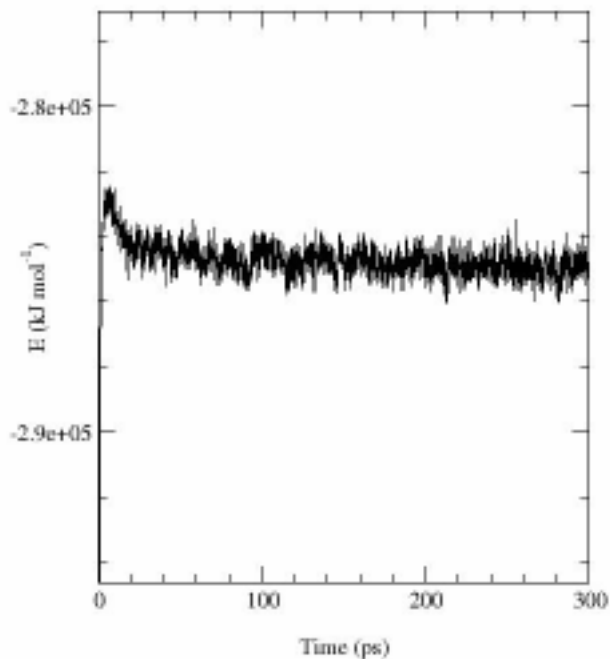
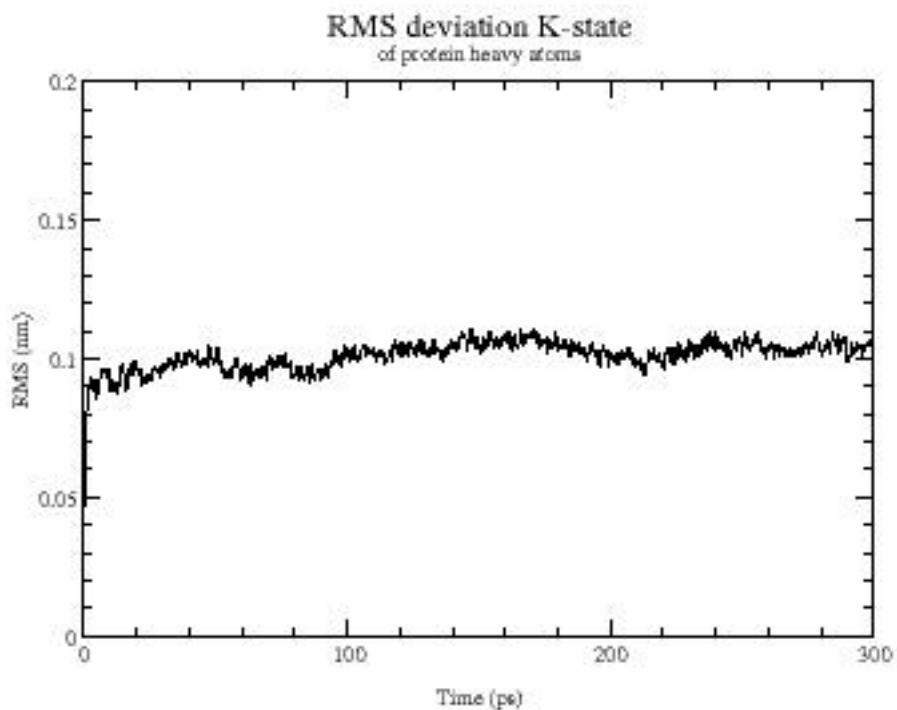Figure 5. Potential energy as a function of time in a K-state simulation.

Figure 6. Root mean square deviation over time of all protein heavy atoms in a K-state simulation, as compared to the crystal structure.

5.2. Hydrogen-Bond Networks

An average structure of each state was calculated and minimised, and then used to map the respective hydrogen-bond patterns. The average structures are presented in figure 7, 8 and 9 (ground-, K-, and L-state, respectively), showing the pore surrounded by helices C, D, F and G, the retinal molecule, K216, and water molecules which are stable in the pore throughout the simulations. The water molecules which are referred to in this discussion are labeled. Potential hydrogen-bonds were calculated using GROMACS (van der Spoel et al. 1996) and plotted in the models, the network of the K intermediate is shown in figure 10. Potential hydrogen-bonds in the three different states are tabulated in table 1, 2 and 3, respectively.

Table 1. **Ground-state**. Hydrogen-bonding pattern for the average ground-state structure. X denotes one potential hydrogen-bond between residues, XX two bonds. The water-numbering is given in figure 8.

residues	donor	45	46	57	82	85	86	89	96	185	216	W400	W402	W403	D1	D2	D4
acceptor																	
41		X															
42			X														
46									X								
57					X									X			
82																	
85							X				X						
92									X								
96																	X
204																	
205																	
212				X			X			X	X	X					
W400					X												
W402														X			
W403					XX												
D2																	
D3					X												
D5					X												

Table 2. **K-state.** Hydrogen-bonding pattern for the average K-state structure. X denotes one potential hydrogen-bond between residues, XX two bonds. The water-numbering is given in figure 9.

residues	donor	45	46	57	82	85	86	89	96	185	216	W400	W402	W403	D1	D2	D4
acceptor																	
41																	
42			X														
46																	X
57					X												
82						X											
85					X			X				XX					
92									X								
96																	
204																	
205																	
212							X			X	X						
W400																	
W402																	
W403																	
D2																	
D3																	
D5																	

Table 3. **L-state.** Hydrogen-bonding pattern for the average L-state structure. X denotes one potential hydrogen-bond between residues, XX two bonds. The water-numbering is given in figure 10.

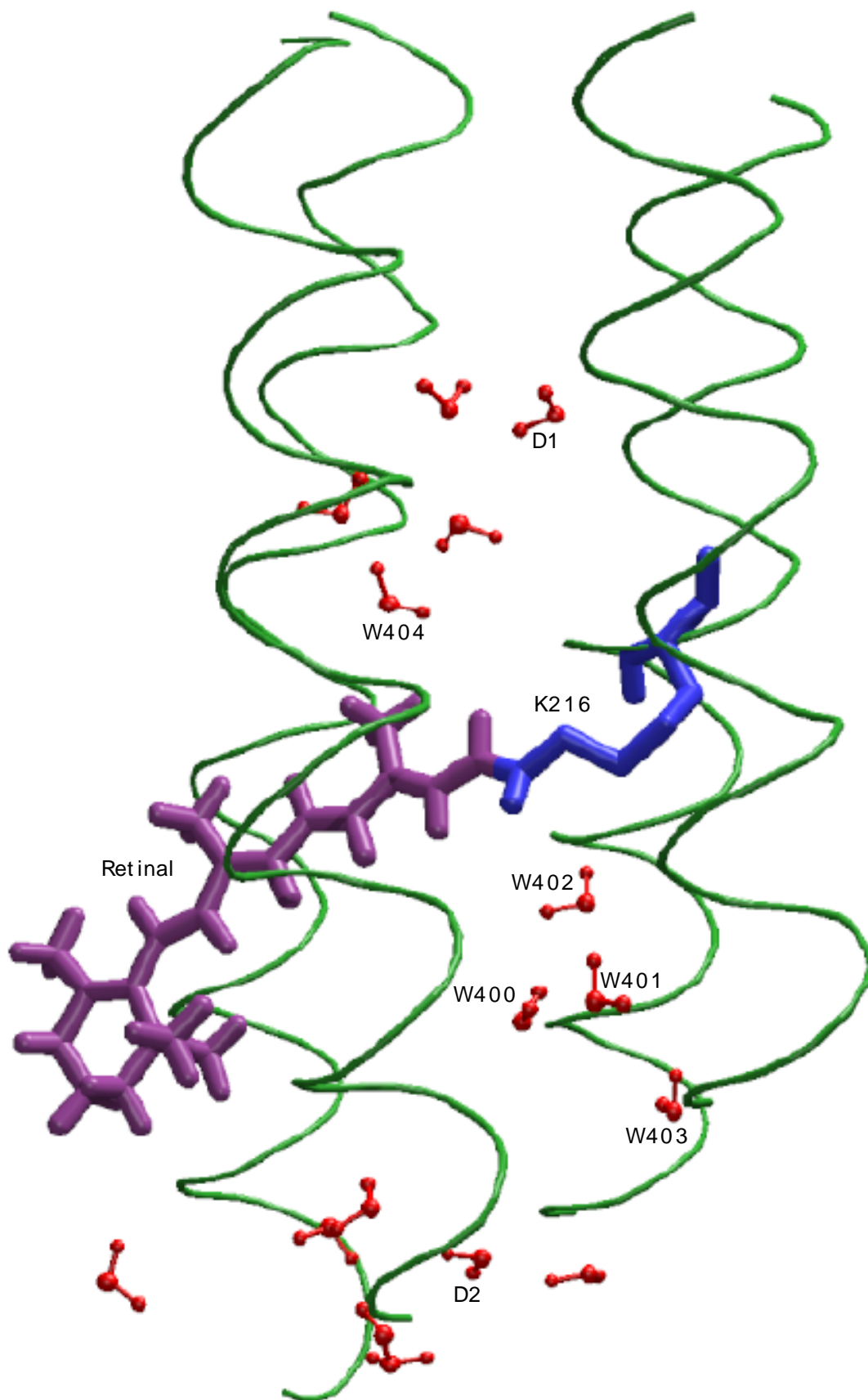| residues	donor	45	46	57	82	85	86	89	96	185	216	W400	W402	W403	D1	D2	D4
acceptor																	
41																	
42			X														
46																X	
57												X					
82																	
85								X									
92									X								
96																	
204					X										X		
205												X					
212							X			X	X			X			
W400					X												
W402																	
W403																	
D2									X								
D3					XX												
D5																	

Figure 7. Helices B, C, F and G of the average simulated ground-state structure. The numbered waters are potentially involved in hydrogen-bonding, or mentioned in the discussion. Waters introduced by Dowser are denoted D, the others are numbered according to Edman et al. 1999.
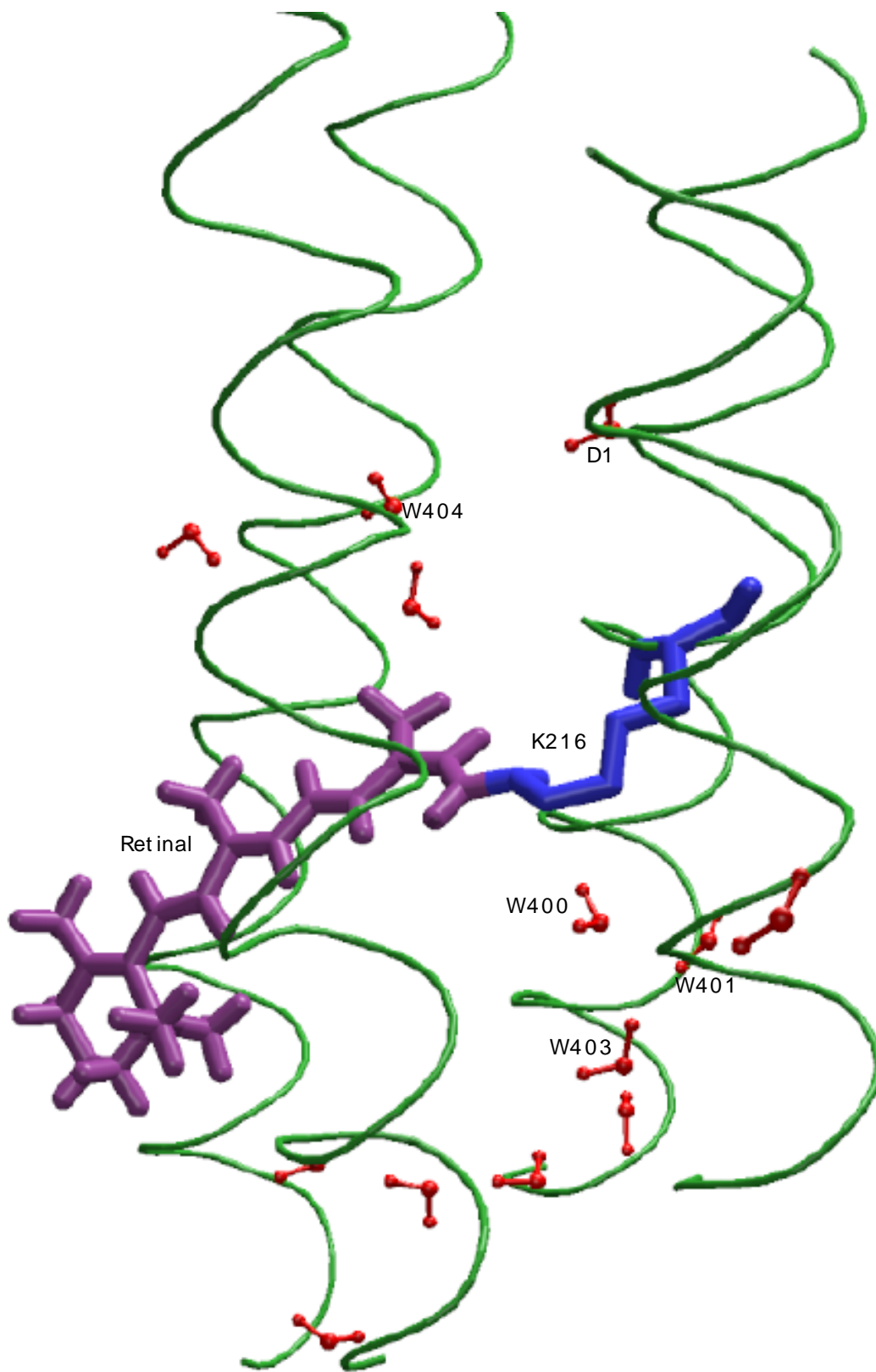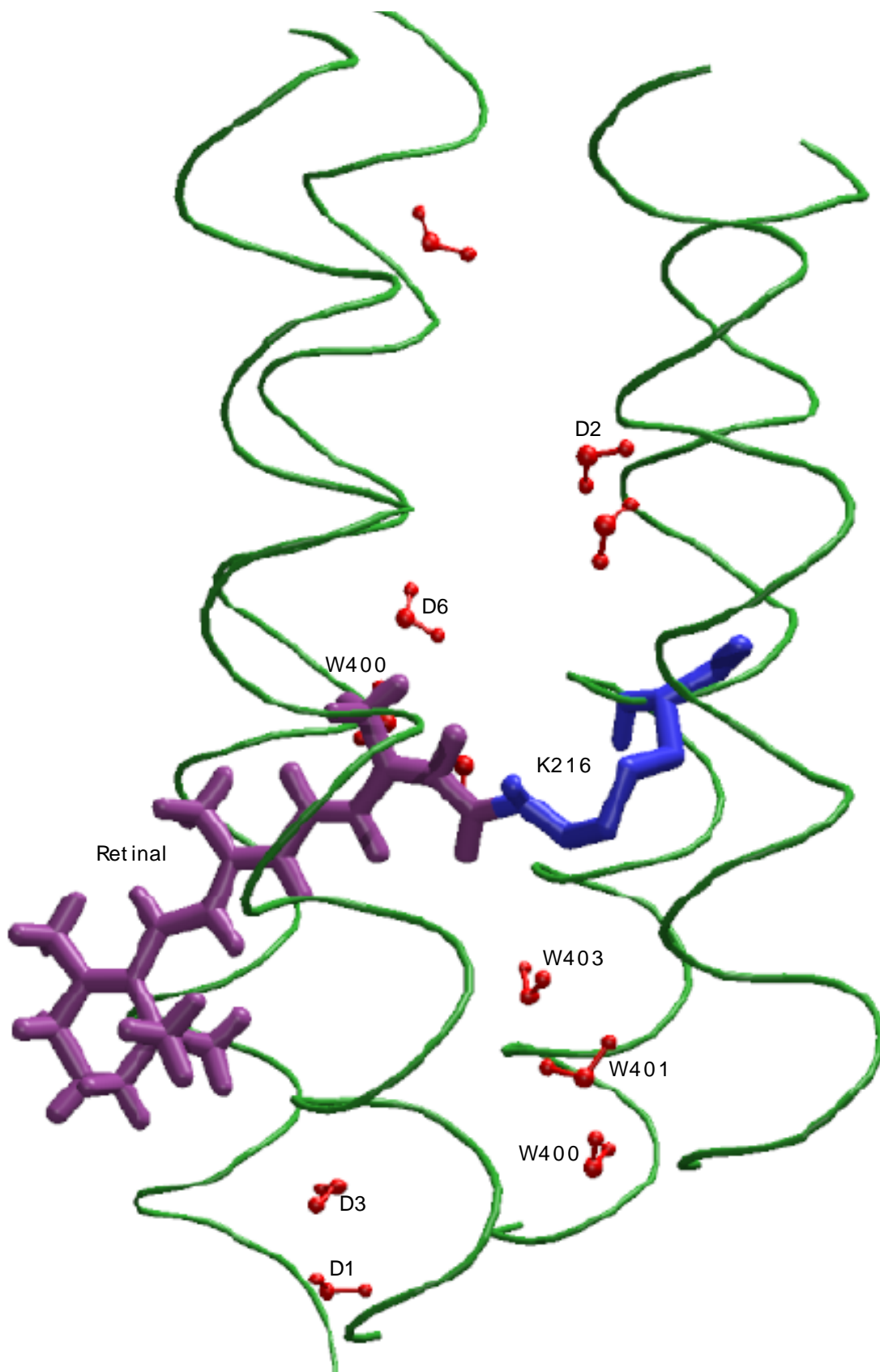
Figure 8. Helices B, C, F and G of the average simulated K-state structure. The numbered waters are potentially involved in hydrogen-bonding, or mentioned in the discussion. Waters introduced by Dowser are denoted D, the others are numbered according to Edman et al. 1999.

Figure 9. Helices B, C, F and G of the average simulated L-state structure. The numbered waters are potentially involved in hydrogen-bonding, or mentioned in the discussion. Waters introduced by Dowser are denoted D, the others are numbered according to Edman et al. 1999.
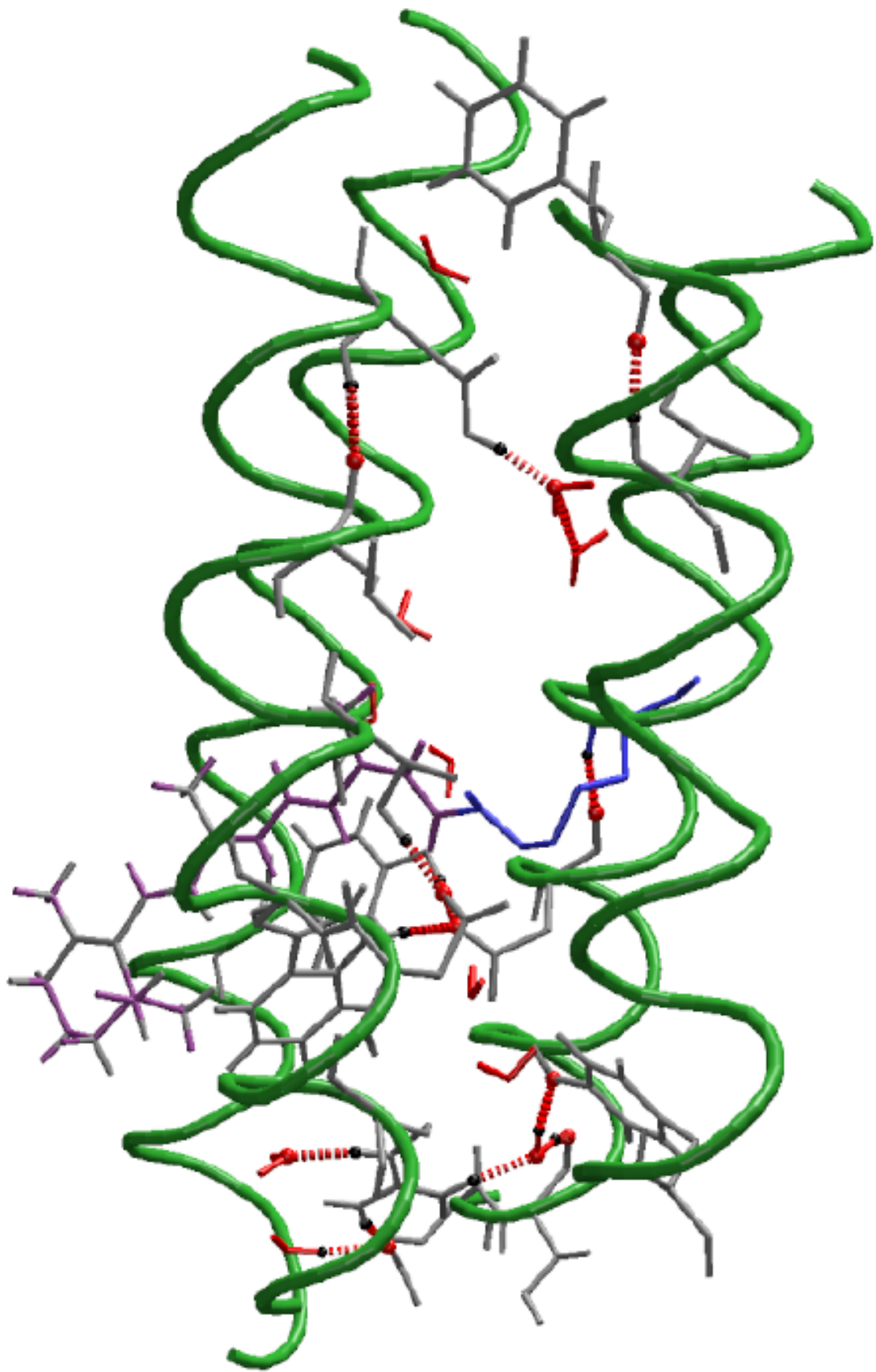
Figure 10. Helices B, C, F and G of the average simulated K-state structure. The potential hydrogen-bonding network in the channel is mapped in red.

In figure 10 it is shown that there is no continuous proton path from the cytoplasmic to the extracellular side in the average K-state structure, which is also the case for the ground- and L-states. A possible reason for this is that we are looking at an average structure, the individual structures of the trajectory are slightly different, and the atomic fluctuations can lead to the breakage and reformation of hydrogen-bonds over time. In the case of the water molecules this is especially true, as they are more free to move around. Another possibility is that one or several water molecules are missing in our starting models. It has also been suggested that a directed random walk by one water molecule through the pore could deliver the proton (Sass et al. 2000), however, this theory is not supported by our simulations.

5.2.1. Ground state

The most interesting feature of the average ground state structure is in the chromophore region. The crystal structure shows W402 co-ordinated between the Schiff base and the two aspartic acid residues, D85 and D212. In our average structure the nitrogen of the Shiff base points towards OD2 of D85, the distance being 3.5 Å between them. The water molecule (W402) is positioned between the two aspartic acids, but not hydrogen-bonded to them, and is stable in this position throughout the simulation. There is clearly an attractive force between the charged Schiff base and the aspartic acid, but whether this conformation is more stable than the crystal structure conformation is uncertain. If the water position of our average structure is correct, it might indicate that a direct proton transfer later in the photocycle is more likely than a water mediated transfer. The root mean square deviation (rmsd) between the average structure and the crystal structure of the ground state is 1.1 Å for protein heavy atoms, and 0.2 Å for the retinal molecule (all atoms).

5.2.2. K intermediate

The average K-state structure agrees well with the crystal structure (rmsd 0.9 Å for protein heavy atoms). However, W400 (numbering according to Edman et al. 1999) moves about 4 Å from the crystal position below the aspartic acids D85 and D212 up towards the ground state position of W402, but to a position about 1 Å further away from the Schiff base (see figures 7 and 8). It is hydrogen-bonded to D85, but neither W400 nor D85 is in contact with the Schiff base. Also, W401 is rather mobile in the simulation. When considering these movements, it should be kept in mind that both W400 and W401 are dislocated in the crystal structure of the following intermediate, the L-state (Royant et al. 2000). It is clear that the waters in general move around more in the K-state than in simulations of the other two states. The hydrogen-bonding pattern for the K-state (table 2) is less extensive than that of both the ground- (table 1) and the L-state (table 3)

average structures. This can be related to the fact that the K intermediate has a shorter lifetime, and is therefore less stable, than the L intermediate (figure 2). The Schiff base, although it fluctuates a lot, points towards the cytoplasmic side and away from D85 throughout the simulation, and in agreement with expectations there is no apparent route for proton transfer during this stage of the photocycle.

5.2.3. L intermediate

The hydrogen-bonding network for the average L-state structure is described in table 3 and water positions are given in figure 9. The root mean square deviation between the average structure and the crystal structure of the L intermediate is 1.1 Å for protein heavy atoms. One striking difference is the position of the Schiff base, which in the average structure is twisted towards the aspartic acid D85, the primary proton acceptor. A close-up of the average L-state structure is viewed in figure 11, with the Schiff base – D85 contact indicated. The average distance between these two atoms over the trajectory is 3.3 Å. During the simulation the Shiff base fluctuates, and is in hydrogen-bonding position with D85 at certain times. The whole complex is further stabilised by a water molecule interacting with D212, at the position of the 'new' water molecule that appears at the centre of W400, W401 and W402 in the L-state crystal structure of Royant et al. 2000, which they have labelled W401 (see figure 3). Early in our simulation W401 and W403 swap positions, as is apparent from the numbering in figure 9, but taken together the two water positions are close to those in the crystal structure. A similar exchange of positions take place between W404 and a water introduced by Dowser, D6. These results suggest that the structure is "loose" at this stage, and water diffusion can readily be achived.

5.2.4. Proton transfer

Our results show that a proton is transferred directly from the Schiff base to the aspartic acid D85. This direct proton transfer model is also supported by the fact that the transfer is a one-step kinetic reaction (Luecke et al. 2000). It seems unlikely that W402, or some other water taking its place, is involved in the transfer process, as it is not present in the average L-state structure, and W400 in the average K-state structure is too far away to interact with the Schiff base and D85. However, there is room for a water molecule in the cavity between the Schiff base, T89 and D85, and a water placed in this position in an L-state simulation is stable for some time. Based on our data it is not as yet possible to say whether this is an alternative to the direct transfer model. The difference in the Schiff base behaviour between the K- and L-state simulations can be due to the crystallographically resolved structural changes in the transition between the two states, where helices C and G are shifted in the L-state relative to their K-state positions.
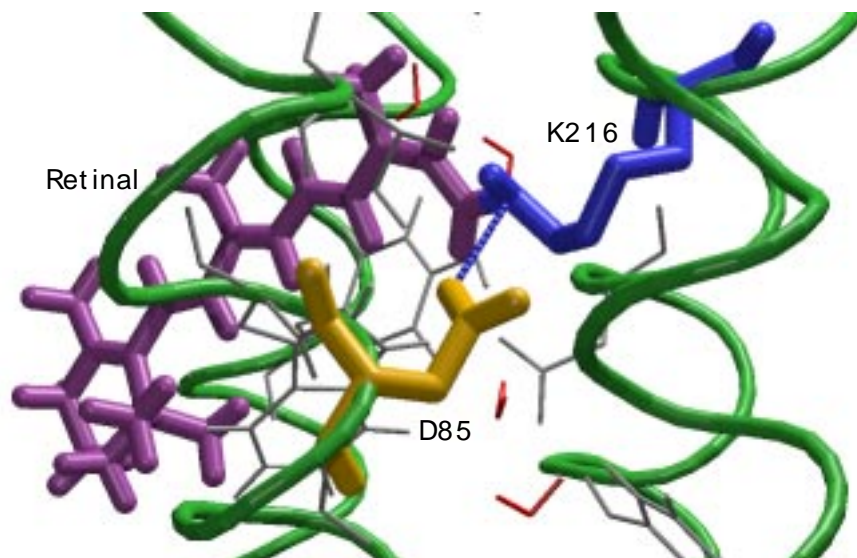
Figure 11. Close-up of the retinal vicinity in the average simulated L-state structure. The potential direct proton transfer pathway between the Schiff base nitrogen and the closest oxygen of D85 is indicated as a purple line.

6. CONCLUSIONS

This work provides support for the view that reorganisation of internal water molecules is crucial for proton pumping in bacteriorhodopsin. We have shown that the hydrogen-bonding patterns are different between the ground-, K- and L-states, although we cannot see continuous paths. Analysing the separate structures of the trajectories might provide additional information, as opposed to just looking at average structures as was done here.

One powerful feature of molecular dynamics simulations is the possibility of looking at dynamic events, which was important in this study. We see major fluctuations of the Schiff base in the simulation of the K- as well as of the L intermediate, but in different directions. The approach of the Schiff base nitrogen towards the aspartic acid residue D85 in the L-state simulation, indicate that the primary proton transfer is direct.

7. ACKNOWLEDGEMENTS

8. REFERENCES

Bashford, D. and Gerwert, K. *Electrostatic calculations of the pK$_a$ values of ionizable groups in bacteriorhodopsin*. J. Mol. Biol. **224**, 473-486 (1992)

Baudry, J., Tajkhorshid, E., Molnar, F., Phillips, J. and Schulten, K. *Molecular dynamics study of bacteriorhodopsin and the purple membrane*. J. Phys. Chem. B **105**, 905-918 (2001)

Belrhali, H., Nollert, P., Royant, A., Menzel, C., Rosenbusch, J. P., Landau, E. M. and Pebay-Peyroula, E. *Protein, lipid and water organization in bacteriorhodopsin: a molecular view if the membrane at 1.9 angstroms resolution*. Structure (London) **7**, 909 (1999)

Berendsen, H. J. C., Postma, J. P. M., Gunsteren, W. F. and Hemans, J. *Interaction models for water in relation to protein hydration*. Intramolecular forces; Pullman, B., Ed.; Reidel: Dordrecht, The Netherlands, pp 331-342 (1981)

Braiman, M. and Mathies, R. *Resonance Raman spectra of bacteriorhodopsin's primary photoproduct: Evidence for a distorted 13-cis retinal*. Proc. Natl Acad. Sci. USA **79**, 403-407 (1982)

Darden, T., York, D. and Pedersen, L. *Particle mesh Ewald: An N-log(N) method for Ewald sums in large systems*. J. Chem. Phys. **98**, 10089-10092 (1993)

Edman, K., Nollert, P., Royant, A., Belrhali, H., Pebay-Peyroula, E., Hajdu, J., Neutze, R. and Landau, E. *High-resolution x-ray structure of an early intermediate on the bacteriorhodopsin photocycle*. Nature **401**, 822-826 (1999)

Gerwert, K., Hess, B., Soppa, J. and Oesterhelt, D. *Role of Asp-96 in proton translocation by bacteriorhodopsin*. Proc. Natl. Acad. Sci. USA **86**, 4943-4947 (1989)

Haupts, U., Tittor, J. and Oesterhelt, D. *Closing in on bacteriorhodopsin.* Annu. Rev. Biophys. Biomol. Struct. **28**, 367-399 (1999)

Hermone, A. and Kuczera, K. *Free-energy simulations of the retinal cis→ trans isomerization in bacteriorhodopsin*. Biochemistry **37**, 2843-2853 (1998)

Henderson, R. and Unwin, P. N. T. *Three dimensional model of purple membrane obtained by electron microscopy*. Nature **257**, 28-32 (1975)

Hess, B., Bekker, H., Berendsen, H. J. C. and Fraaije, J. G. E. M. *LINCS: A linear constraint solver for molecular simulations*. J. Comput. Chem. **18**, 1463-1472 (1997)

Herberle, J., Fitter, J., Sass, H. and Büldt, G. *Bacteriorhodopsin: the functional details of a molecular machine are being resolved*. Biophys. Chem. **85**, 229-248 (2000)

Humphrey, W., Xu, D., Sheves, M. and Schulten, K. *Molecular dynamics study of the early intermediates in the bacteriorhodopsin photocycle*. J. Phys. Chem. **99**, 14549-14560 (1995)

Humphrey, W., Dalke, A. and Schulten, K. *VMD – Visual Molecular Dynamics*. J. Molec. Graphics **14.1**, 33-38 (1996)

Humphrey, W. and Schulten, K. *Photoproducts of bacteriorhodopsin mutants: a molecular dynamics study*. Biophys. J. **72**, 1347-1356 (1997)

Humphrey, W., Lu, H., Logunov, I., Werner, H.-J. and Schulten, K. *Three electronic state model of the primary phototransformation of bacteriorhodopsin*. Biophys. J. **75**, 1689-1699 (1998)

Kühlbrandt, W. *Bacteriorhodopsin – the movie*. Nature **406**, (2000)

Lanyi, J. *Progress toward an explicit mechanistic model for the light-driven pump, bacteriorhodopsin*. FEBS Letters **464**, 103-107 (1999)

Luecke, H., Schobert, B., Richter, H. T., Cartailler, J.-P. and Lanyi, J. K. *Structure of bacteriorhodopsin at 1.55 A resolution*. J. Mol. Biol. **291**, 899-911 (1999a)

Luecke, H., Schobert, B., Richter, H. T., Cartailler, J.-P., and Lanyi, J. *Structural changes in bacteriorhodopsin during ion transport at 2 Å resolution*. Science **286**, 255-260 (1999b)

Luecke, H., Schobert, B., Cartailler, J.-P., Richter, H. T., Rosengarth, A., Needleman, R. and Lanyi, J. *Coupling photoisomerization of retinal to directional transport in bacteriorhodopsin*. J. Mol. Biol. **300**, 1237-1255 (2000)

Merritt, E. A. and Bacon, D. J. *Raster3D: Photorealistic molecular graphics*. Method Enzymol. **277**, 505-524 (1997)

Royant, A., Edman, K., Ursby, T., Pebay-Peyrouls, E., Landau, E. and Neutze, R. *Helix deformation is coupled to vectorial proton transport in the photocycle of bacteriorhodopsin*. Nature **406**, 645-648 (2000)

Sass, H., Büldt, G., Gessenich, R., Hehn, D., Neff, D., Schlesinger, R., Berendzen, J. and Ormos, P. *Structural alterations for proton translocation in the M state of wild-type bacteriorhodopsin*. Nature **406**, 649-653 (2000)

Subramaniam, S. and Henderson, R. *Molecular mechanism of vectorial proton translocation by bacteriorhodopsin*. Nature **406**, 653-657 (2000)

Tajkhorshid, E., Paizs, B. and Suhai, S. *Conformational effects on the proton affinity of the Schiff base in bacterirhodopsin: a density functional study*. J. Phys. Chem. B **101**, 8021-8028 (1997)

Tajkhorshid, E. and Suhai, S. *The effect of the protein environment on the structure and charge distribution of the Schiff base in bacterirhodopsin*. Theor. Chem. Acc. **101**, 180-185 (1999a)

Tajkhorshid, E. and Suhai, S. *Influence of the methyl groups on the structure, charge distribution, and proton affinity of the retinal Schiff base*. J. Phys. Chem. B **103**, 5581-5590 (1999b)

van de Spoel, D., van Buuren, A. R., Apol, E., Meulenhoff, P. J., Tielman, D. P., Sijbers, A. L. T. M., Hess, B., Feenstra, K. A., Lindahl, E., van Drunen, R. and Berendsen, H. J. C. *Gromacs 2.0 Manual*. University of Groningen, Groningen, The Netherlands. Internet: http://rugmd0.chem.rug.nl/~gmx (1996)

van Gunsteren, W. F., Billeter, S. R., Eising, A. A. and Hunenberger, P. H. H. Biomolecular Simulation: *The GROMOS96 manual and user guide*. Hochschukverlag AG an der ETH Zurich, Zurich, Switzerland

Vonck, J. *Structure of the bacteriorhodopsin mutant F212L intermediate revealed by electron crystallography*. EMBO J. **19**, 2152-2160 (2000)